The old and new Concepts of Physics
An open-dialogue journal

www.uni.lodz.pl/concepts

HEAVY AND SUPERHEAVY ATOMIC NUCLEI

Adam Sobiczewski
Soltan Institute for Nuclear Studies
Hoża 69, 00-681 Warsaw, Poland
e-mail:adam.sobiczewski@fuw.edu.pl

(Received 9 May 2008; accepted 3 June 2008)

Abstract

The appearance and development of the concept of superheavy atomic nuclei are described. The concept appeared during the studies of the limits of the nuclear chart and of the periodic table of the chemical elements. The article concentrates on theoretical studies of the properties of heaviest nuclei. Results of these studies are illustrated and discussed. Prospects for a nearest future of the research of heaviest nuclei are outlined.

DOI: 10.2478/v10005-007-0047-2

1 Introduction

The heaviest element which appears in the Earth in the natural way is uranium (the atomic number Z=92). All heavier ones had to be produced artificially in nuclear reactions. Production of them is a long and fascinating story (since 1940, when the first of them, neptunium (Np, Z=93) has been obtained, see e.g. [1]). Presently, all the elements with Z from Z=93 to Z=118, with the only exception of Z=117, are already known. Description of the synthesis of them may be found e.g. in the papers [2–7] and in the references given therein.

A fundamental problem of heaviest nuclei is to determine the largest proton, Z, and neutron, N, numbers with which they can exist and can be synthesized. For a long time, when one did not realize of the shell structure of a nucleus, nobody was expecting nuclei with Z larger than about 100 to exist. Only the discovery of this structure has opened a chance for existence of such nuclei. Especially privileged, strongly bound, are the nuclei with a closed proton or neutron shell (so called magic nuclei) and, particularly, the nuclei with both shells closed (doubly magic nuclei). The main scope of the theory of heaviest nuclei is just to study their shell structure and effects of this structure in their properties, particularly in their half-lives and in the cross sections for their synthesis.

According to calculations, all nuclei with Z larger than about 103 (i.e. the transactinide nuclei) exist only due to their shell structure. Without this structure, they would not exist. These nuclei are called superheavy nuclei (SHN) and the respective elements are called superheavy elements (SHE).

Specific properties of heaviest nuclei are their short half-lives (usually of the order of seconds and below) and small cross sections for their synthesis. As the result, one cannot collect them. Before producing a new nucleus, the previous one already decayed. Thus, physics of heaviest nuclei is the physics of single nuclei and chemistry of heaviest elements is the chemistry of single atoms.

The objective of this paper is a discussion of the appearance and development of the concept of superheavy nuclei. These are directly connected with the studies of heaviest nuclei. The results of these studies are illustrated and discussed. Main attention is given here to theoretical studies of the properties of these nuclei. Theoretical studies of the cross sections for their synthesis are described in a separate article [8]. A review of the experimental research on the heaviest nuclei is given in [9].

2 Theoretical methods

There exist two main approaches in the theoretical description of nuclei. One, traditional, is a macroscopic-microscopic (macro-micro) approach (e.g. [10–14]), the other, more recent, are purely microscopic, self-consistent methods. The self-consistent methods use calculations of the Hartree-Fock type with effective density-dependent interactions of the zero-range (Skyrme) type (e.g. [15, 16]) or of the finite-range (Gogny) type (e.g. [17, 18]). To the purely microscopic methods, belongs also the relativistic mean field approach (e.g. [19–21]) intensively used in recent years in the description of nuclear properties. A recent review of both macro-micro and self-consistent methods and the results obtained with the use of them is given in [22].

To illustrate the description of heaviest nuclei, we will mainly use the results obtained within a macroscopic-microscopic approach. In this approach, the energy (mass) of a nucleus is composed of two parts: macroscopic and microscopic. The macroscopic part, which smoothly depends on the proton Z and neutron N numbers, does not include effects of the shell structure of a nucleus. It is usually described by such models as the liquid-drop one (e.g. [23, 24]) or the Yukawa-plus-exponential model [25]. The microscopic part describes shell effects. It usually bases on a realistic single-particle nuclear potential (most often the Woods-Saxon potential [26]) and is constructed from the single-particle energy spectra by the Strutinski procedure [27].

3 Shell effects and their role in the stability of heaviest nuclei

Effects of shell structure are important for all nuclei. Their role for the heaviest ones is, however, essential because these nuclei would not exist without these effects [28], as already mentioned in the Introduction. In this section, we will illustrate this role in a number of properties of heavy and superheavy nuclei.

Figure 1 [28] illustrates shell effects in masses of heaviest nuclei. The effect is the difference between the experimental value of mass and the value calculated within a model which does not contain shell structure (e.g., liquid-drop model). One can see that the shell effect, $M^{\mathrm{exp}} - \tilde{M}$, is negative (i.e., stabilizes the nuclei) and decreases (increases in its absolute value) with increasing atomic number Z, down to about -5 MeV for the heaviest even-even nuclei ^{260}Sg (Z=106) and ^{264}Hs (Z=108), known at the time when early studies of shell effects in the properties of heaviest nuclei were done. The effect of the known deformed shell at the neutron number N=152 is clearly seen in the results for Cf, Fm and No (Z=102) isotopes. Similarly clear and large shell effects were found in other important properties of heaviest nuclei, such as the α-decay energy Q_α and half-life T_α or the height of the fission barrier B_{f} [28].

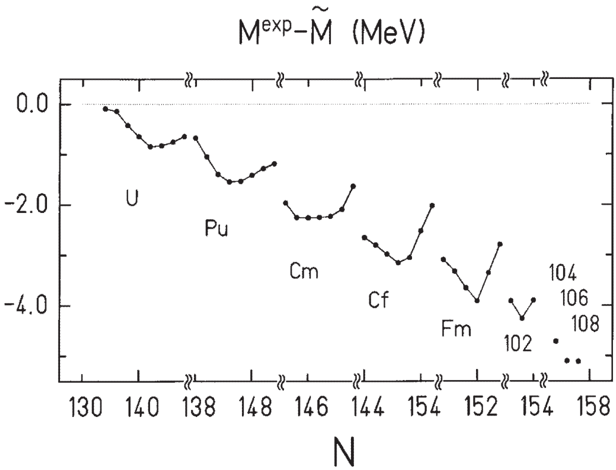

Figure 1: Shell effects in the masses of nuclei [28].

An especially large effect, up to 15 orders of magnitude, appears in the spontaneous-fission half-life T_{sf}. This is because this quantity is especially sensitive to the shell structure of a nucleus. The effect is illustrated in Fig. 2 [28]. The figure shows the experimental (exp) and theoretical (Y) values of the logaritm of T_{sf}. The theoretical values are calculated by a macroscopic (Yukawa-plus-exponential [25]) model, which does not include any shell structure of a nucleus. Thus, the difference between the two values is just the shell effect in the spontaneous-fission half-life T_{sf}. One can see that the effect delays the fission process in all considered nuclei, except only few lightest ones (isotopes of uranium). The delay increases from few orders (Pu isotopes) to about 15 orders of magnitude for the nucleus $^{260}106$ (^{260}Sg), which has the largest Z among the even-even nuclei with measured T_{sf}. For such a heavy nucleus like $^{260}106$, with T_{sf} of the order of few milliseconds, this elongation makes up practically the whole half-life of these nuclei. In other words, they would not exist without shell effects, as already mentioned above.

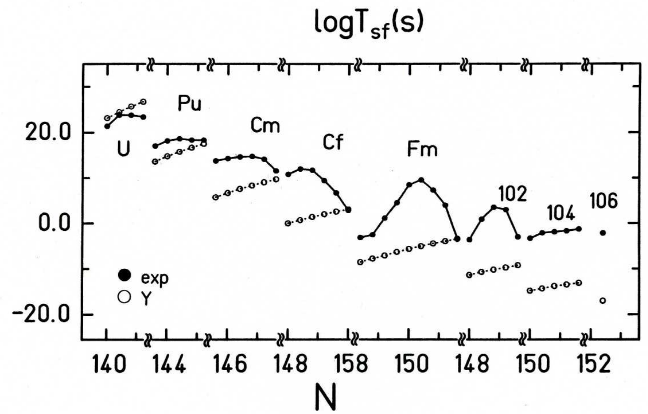

Figure 2: Logarithm of experimental (exp) and calculated macroscopically (Y) spontaneous-fission half-lives T_{sf}, given in seconds [28].

The mechanism by which practically the whole half-life of a very heavy nucleus is made up by shell effects is illustrated in Fig. 3. The figure illustrates the spontaneous-fission barrier of the nucleus $^{264}108$ (^{264}Hs), i.e. the dependence of the ground-state energy of this nucleus on its quadrupole-deformation parameter β_2. For each β_2, the energy is minimized with respect to the hexadecapole-deformation parameter

β_4. The total fission barrier (Y+SHELL), including shell effects, is shown by solid line and its smooth part (obtained by the Yukawa-plus-exponential model (Y) [25]), by dashed line. The smooth barrier obtained by another macroscopic model (liquid drop, LD [23]) is also shown (dotted line), for comparison. One can see that a significant height (about 6 MeV) of the fission barrier is obtained only after the inclusion of shell effects. Without them, no fission barrier (Y and LD) appears.

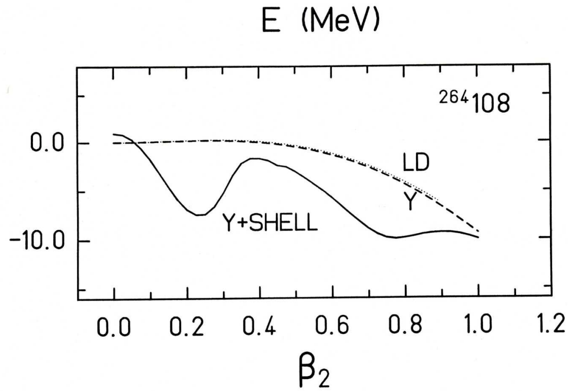

Figure 3: Total fission barrier (Y+SHELL) and its macroscopic part obtained by Yukawa-plus-exponential (Y) and by the liquid-drop (LD) models, for the nucleus $^{264}108$ [28].

To get a first orientation in which nuclei the shell effects are largest, one had to calculate them for a large region of the nuclear chart. This has been done in [29]. The results are shown in Fig. 4 [29]. The figure shows a contour map of the shell correction $E_{\rm sh}$ to the ground-state energy (or mass) of nuclei in a large region of nuclides with proton number Z=82-124 and neutron number N=126-190. One can see that $E_{\rm sh}$ has three minima in this region. The first one, which is the deepest ($E_{\rm sh}$=–14.3 MeV), is obtained for the doubly magic spherical nucleus ^{208}Pb. The second one ($E_{\rm sh}$=–7.2 MeV) appears at the nucleus $^{270}108_{162}$, which is predicted [30, 31] to be a doubly magic deformed nucleus. The third minimum, with the same depth

(E_{sh}=–7.2 MeV) as that of the second one, is obtained for the nucleus $^{296}114_{182}$, which is close to the nucleus $^{298}114_{184}$ predicted [32–34] to be a doubly magic spherical nucleus, the next one to the last experimentally known double-magic ^{208}Pb. Besides these three minima, there appears a rather wide plateau around the nucleus ^{252}Fm, which, although having a smaller (in absolute value) shell correction (E_{sh}=–5.2 MeV) than the nucleus $^{270}108$ (^{270}Hs), may be considered as a nucleus with closed deformed subshells [30, 31].

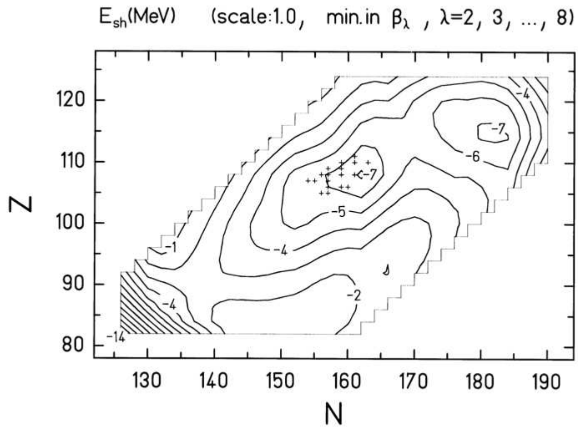

Figure 4: Contour map of the ground-state shell correction energy E_{sh}. Crosses denote heaviest nuclei which were synthesized at the time, when the figure was plotted [29].

One can also see in Fig. 4 that some of the already synthesized nuclei profit by 6-7 MeV in their binding energy from the shell correction. Without this profit they could not exist, as already discussed above.

The appearance of the region of nuclei around the second minimum (deformed superheavy nuclei) constitutes probably the main change in our view of stability of heaviest nuclei in the whole history of SHE. Before this, it was believed for a long time that spherical superheavy nuclei, predicted to be situated around the third minimum, would constitute an island, separated from the usual peninsula of relatively long-lived nuclei by an "ocean" of full instability. After the appearance of deformed superheavy nuclei, however, the peninsula is expected to be extended, to include also the spherical superheavy nuclei. This is qualitatively illustrated in Fig. 5 taken from [35].

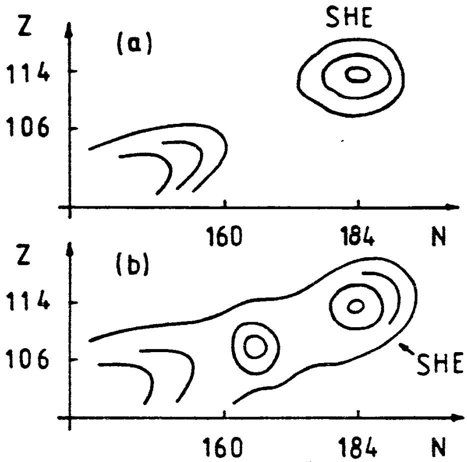

Figure 5: Regions of relatively long-lived heavy nuclei as believed earlier (a), and expected presently (b) [35].

4 Single-particle structure

By single-particle structure of a nucleus, we understand the structure of its single-particle spectrum. The inhomogeneity of the spectrum, the appearance of shells (regions of a larger density of the single-particle energy levels), separated by energy gaps, is just the shell structure of a nucleus.

As large shell corrections to energy (mass) of a nucleus are related to large energy gaps in the single-particle spectra, it is interesting to see the single-particle spectra of the nuclei ^{208}Pb, ^{270}Hs, and ^{298}114, for which the three minima of the shell correction $E_{\rm sh}$ have been

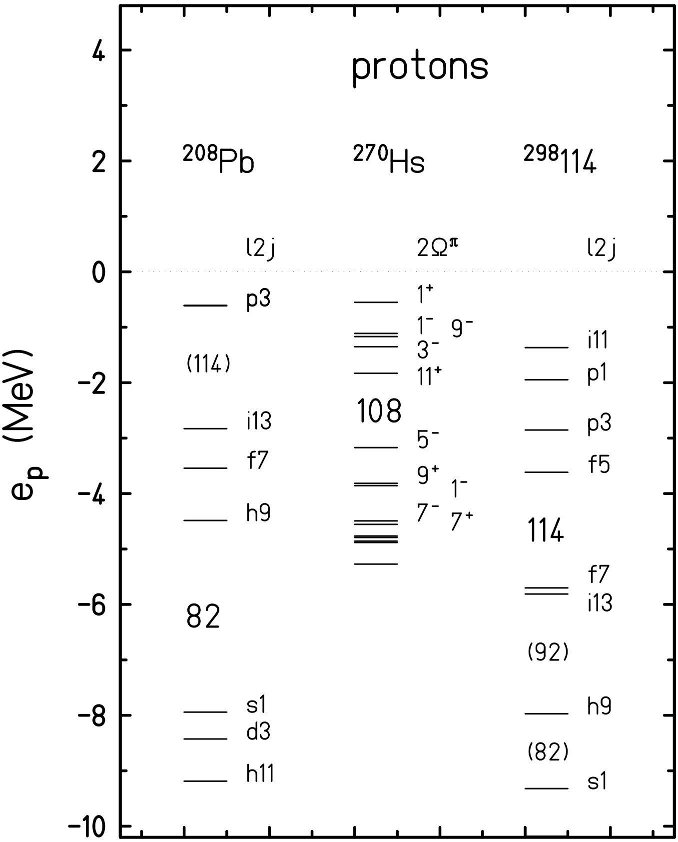

Figure 6: Single-particle proton levels calculated for the doubly magic nuclei ^{208}Pb, ^{270}Hs, and ^{298}114. Spectroscopic symbol for the orbital angular momentum l and total spin (multiplied by two) $2j$ are given at each level of the spherical nuclei ^{208}Pb and ^{298}114. Projection of spin (multiplied by two) 2Ω and parity π are shown at each level of the deformed nucleus ^{270}Hs [36].

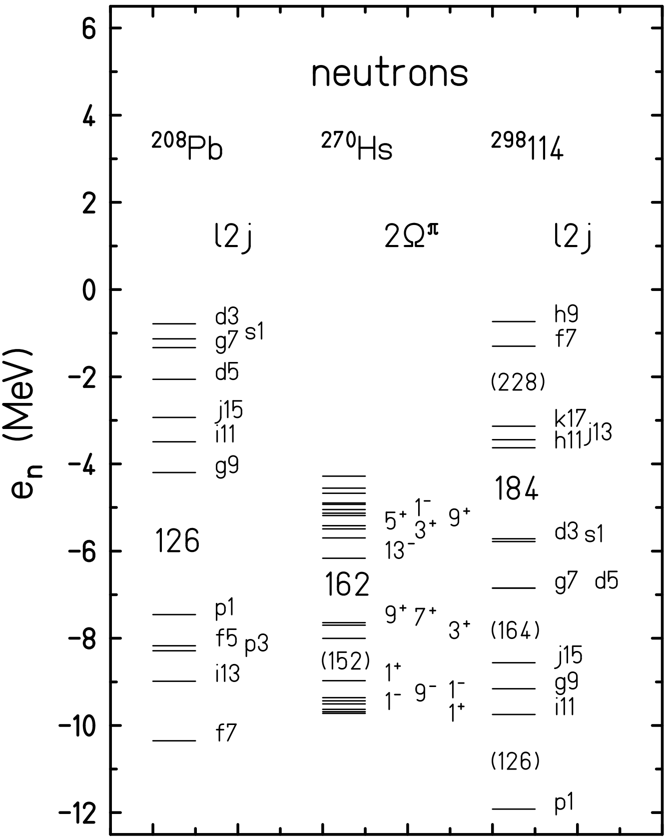

Figure 7: Same as in Fig. 6, but for neutrons [36].

obtained in Fig. 4. The spectra are shown in Fig. 6 for protons and Fig. 7 for neutrons. One can see in Fig. 6 large energy gaps at $Z = 82$ (in the spectrum of ^{208}Pb), at $Z = 108$ (in ^{270}Hs), and at $Z = 114$ (in ^{298}114). In the spectrum of ^{270}Hs, a low density of the levels extends from $Z = 106$ to $Z = 110$. For neutrons, Fig. 7, besides a large energy gap obtained at $N = 162$ in the spectrum of ^{270}Hs, a smaller gap at $N = 152$ is also seen. All these find their reflections in the shell correction to the energy $E_{\rm sh}$ shown in Fig. 4.

5 Illustration of the results on the properties of heaviest nuclei

In this section,we will illustrate some theoretical results for the properties of heavy and superheavy nuclei. The results obtained mainly within a macroscopic-microscopic approach will be given.

5.1 Shapes

Equilibrium shapes of heaviest nuclei are found to be axially symmetric [37]. Thus, they can be described by the usual deformation parameters β_λ, appearing in the following expression for nuclear radius (in the intrinsic frame of reference) in terms of spherical harmonics $Y_{\lambda 0}(\vartheta)$,

$$R(\vartheta) = R_0(\beta_\mu)[1 + \sum_\lambda \beta_\lambda Y_{\lambda 0}(\vartheta)] \ , \tag{1}$$

where the dependence of R_0 on β_μ is determined by the volume-conservation condition.

It is worth mentioning here that the parameters β_λ of Eq. (1), used in macro-micro approaches, describe the shape of the surface of a nucleus (or its equipotential surface). In self-consistent descriptions of the nuclear shape, multipole moments of mass distribution are usually used to parametrize the shape. The relation between the two parametrizations is rather complex. Even in the case of a very simple (uniform with sharp surface) radial distribution of mass, the mass moment of a given multipolarity Q_μ is a function of the surface parameters β_λ of all multipolarities λ (e.g. [38]).

A macro-micro analysis of the equilibrium deformations has shown [39] that it is sufficient to consider the multipolarities up to λ=8. The contribution of λ=9 and 10 is already negligible. The odd multipolarities λ=3,5,7 contribute only to the deformations of light isotopes of elements around radium [39]. Thus, the 4-dimensional deformation space $\{\beta_\lambda\}$, λ=2,4,6,8, has been found to be sufficient for almost all nuclei in the considered region of heaviest nuclei, in which we are usually interested, in particular for all superheavy nuclei [29].

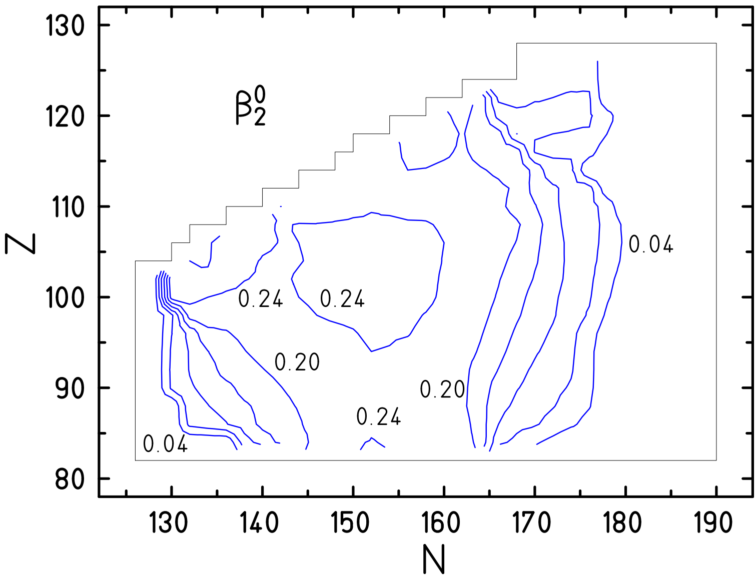

Figure 8: Contour map of the equilibrium deformation β_2^0, plotted as a function of proton (Z) and neutron (N) numbers. Numbers at the contour lines give the values of the deformation [29].

Contour map of the main, quadrupole, component of the equilibrium deformation β_2^0 is given in Fig. 8. The deformation is obtained by minimization of the potential energy of a nucleus in the β_2 degree of freedom. One can see that most of the investigated nuclei are deformed. Only two rather small regions of spherical nuclei appear, one (smaller) around the doubly magic spherical nucleus ^{208}Pb and the other (larger) around the predicted [32–34] strong neutron closed shell at N=184. The main, quadrupole, component of the deformation, β_2^0, is largest and it is positive in almost the whole region of deformed nuclei. It is large ($\beta_2^0 \approx 0.24$) and about constant in a large part of the region (around its center) and it rapidly decreases as one moves towards the boundaries of this region. The higher-multipolarity components are smaller and they change sign as one moves through the region. This situation stresses the important role of these high-multipolarity deformations, as they are mainly responsible for changes of the properties of heavy and superheavy nuclei with changes of Z and N in the large region, where the quadrupole deformation is about constant.

Fig. 9 [40] shows, for comparison, results for β_2^0 obtained within a self-consistent approach (the Hartree-Fock-Bogoliubov method) with the Gogny force. The parameters β_λ are determined here in such a way that the multipole moments Q_μ, calculated with the help of them, and the self-consistent ones are the same. Although the values of β_2^0 are presented here in a different way than in Fig. 8, one can easily see a large similarity between the two.

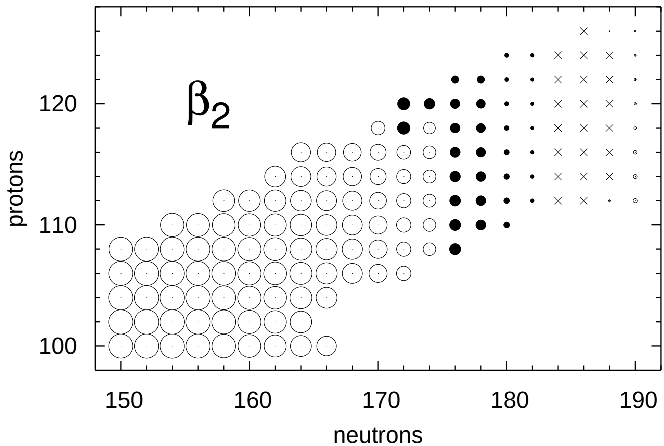

Figure 9: The equilibrium deformation parameter β_2, obtained within the Hartree-Fock-Bogoliubov calculation with the Gogny D1S force. Open circles are used for positive values of the deformations and filled circles for the negative ones. The size of a circle is proportional to the magnitude of the deformation. The covered interval is $-0.181 \leq \beta_2 \leq 0.335$. In the figure, crosses mean $|\beta_2| \leq 0.01$ [40].

The shapes of the nuclei are illustrated in Fig. 10 [41]. Symmetry axes (Oz) of the nuclei have the horizontal orientation in the figure. One can see that the shapes vary quite much with Z and N. Some of the nuclei are thicker in their equatorial plane, some are thinner (necking), some (Z>120) show a tendency to be oblate. Numerical values of the equilibrium deformations β_λ^0, used here, may be found in [42, 43].

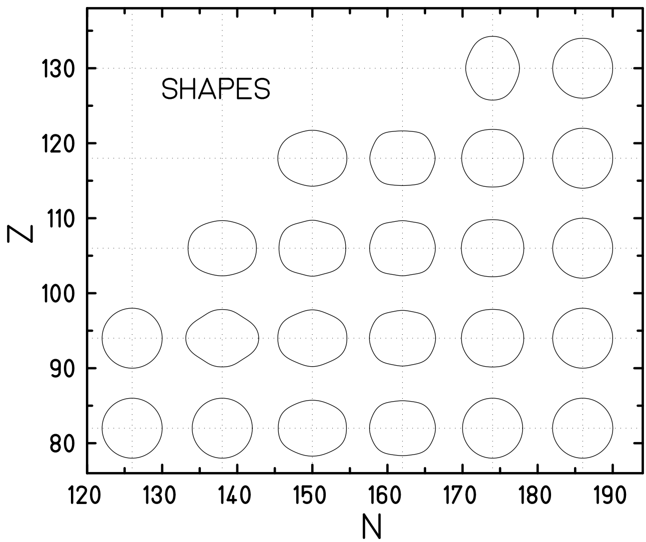

Figure 10: Shapes of nuclei plotted for a wide region of Z=82-130 and N=126-190 [41].

5.2 Deformation energy

To see how well established the deformation is, one should examine the deformation energy, defined as the difference in energy of a nucleus between its spherical and equilibrium shapes, i.e.,

$$E_{\rm def} \equiv E(0) - E(\beta_\lambda^0) \ . \tag{2}$$

Thus, this quantity is the gain in energy of a nucleus due to its deformation. The larger this quantity is, the smaller are the zero-point fluctuations of its shape with respect to its equilibrium shape.

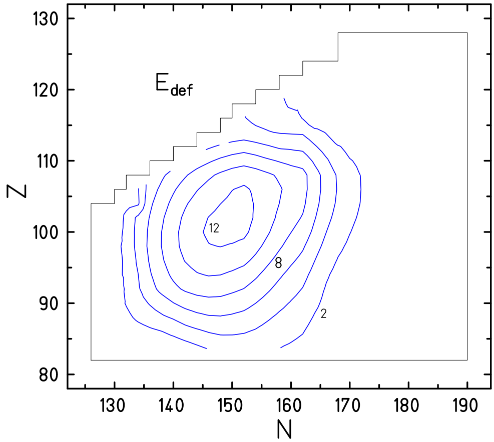

Figure 11: Contour map of the deformation energy $E_{\rm def}$. Numbers at the contour lines give the values of the $E_{\rm def}$ in MeV [41].

The deformation energy, calculated in the region interesting for us, is shown in Fig. 11 [41]. The analysis of this quantity in various nuclei [44] indicates that nuclei with $E_{\rm def} \gtrsim 2$ MeV are well deformed, while those with $E_{\rm def} < 2$ MeV are rather transitional or spherical. One can see in Fig. 11 that most of the considered nuclei are well deformed. The largest values of $E_{\rm def}$ (above 12 MeV) are obtained for nuclei around the nucleus ^{254}No, i.e., for nuclei with the largest quadrupole deformation β_2^0.

It is interesting to see the contribution of deformations of consecutive multipolarity λ to $E_{\rm def}$, in particular of higher λ, and the convergence of $E_{\rm def}$ with increasing λ. Fig. 12 [30] illustrates this in the case of the nucleus ^{252}Fm. Here, $\lambda_{\rm max}$ is the maximal multipolarity of the deformations included to the deformation space $\{\beta_\lambda\}$, λ=2,4,...,$\lambda_{\rm max}$, in which the energy $E_{\rm def}$ is analyzed. One can see

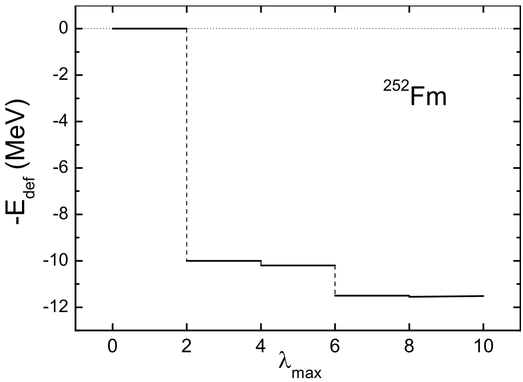

Figure 12: Dependence of the deformation energy (taken with minus sign), $-E_{\rm def}$, on $\lambda_{\rm max}$ for the nucleus ^{252}Fm [30].

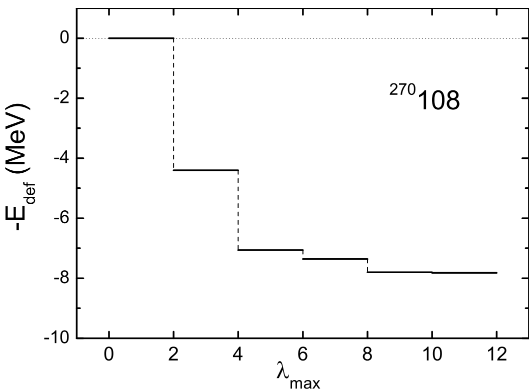

Figure 13: Same as in Fig. 12, but for the nucleus ^{270}Hs [30].

that the quadrupole deformation, β_2, decreases the energy of ^{252}Fm by about 10 MeV, the inclusion of the hexadecapole deformation, β_4, lowers it only very little, while the inclusion of the deformation

β_6 decreases it rather much again (by about 1.3 MeV). Then, the energy appears to be stable with respect to inclusion of still higher deformations. Thus, Fig. 12 stresses the importance of β_6 (i.e., the deformation of a relatively high multipolarity) for such heavy nuclei as the nucleus ^{252}Fm, illustrating simultaneously the convergence of the energy of a nucleus at its equilibrium, as a function of the multipolarity λ_{max}. The examination of another nucleus (^{270}108), Fig. 13, confirms this convergence. Still, different dependences of E_{def} on λ_{max} for these two nuclei stress the individuality of each nucleus, which should be kept in mind when studying them.

5.3 Masses and α-decay energies

Mass is a basic property of a nucleus and it should be described as accurately as possible. Fig. 14 [42] shows the difference between calculated and experimental masses of nuclei with $Z = 94 - 108$. A large, 7-dimensional deformation space $\{\beta_\lambda\}$, λ=2,3,...,8, has been used in the calculations. The large space, including also the odd multipolarities λ=3,5,7, has been used because a large region of nuclei, which also includes relatively light ones (starting from polonium, Z=84) has been considered. For these relatively light nuclei, the odd-multipolarity deformations play a role, as mentioned already above. One can see that the discrepancy between the calculated mass M_{th} and the experimental one M_{exp} is contained within the range of about $\pm$0.5 MeV. Calculated masses show a very good isotopic dependence. This is especially well seen in the long chain of masses of well deformed plutonium nuclei. From masses of Cm, Cf and Fm, one can see that the effect on the mass of the deformed shell at N=152 is well reproduced. One cannot say, however, if this is also the case for a stronger deformed shell at N=162, predicted by theory, because masses of nuclei with N around 162 are not yet measured.

It is interesting to compare the accuracies of descriptions of masses of heaviest nuclei reached within various approaches. Fig. 15 [45] shows the differences $M_{\mathrm{th}} - M_{\mathrm{exp}}$ obtained with the use of a semi-empirical (SE), two macro-micro (HN and TF) and purely microscopic (HF) approaches. The SE description [46] uses a shell model with 15 adjustable parameters, specially adapted to describe masses of nuclei with proton number contained between known magic num-

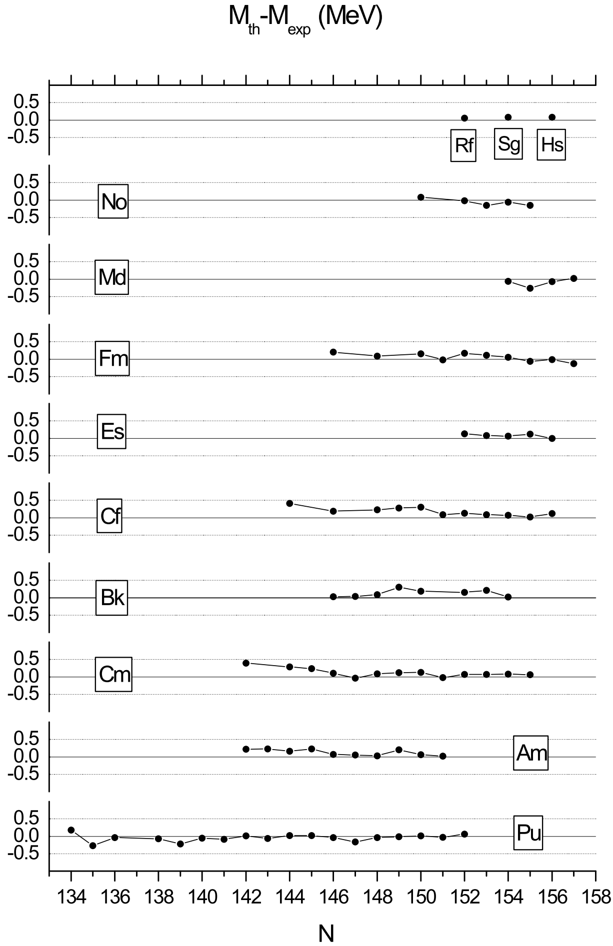

Figure 14: Difference between calculated, $M_{\rm th}$, and measured, $M_{\rm exp}$, masses of nuclei with proton number Z=94-108 [42].

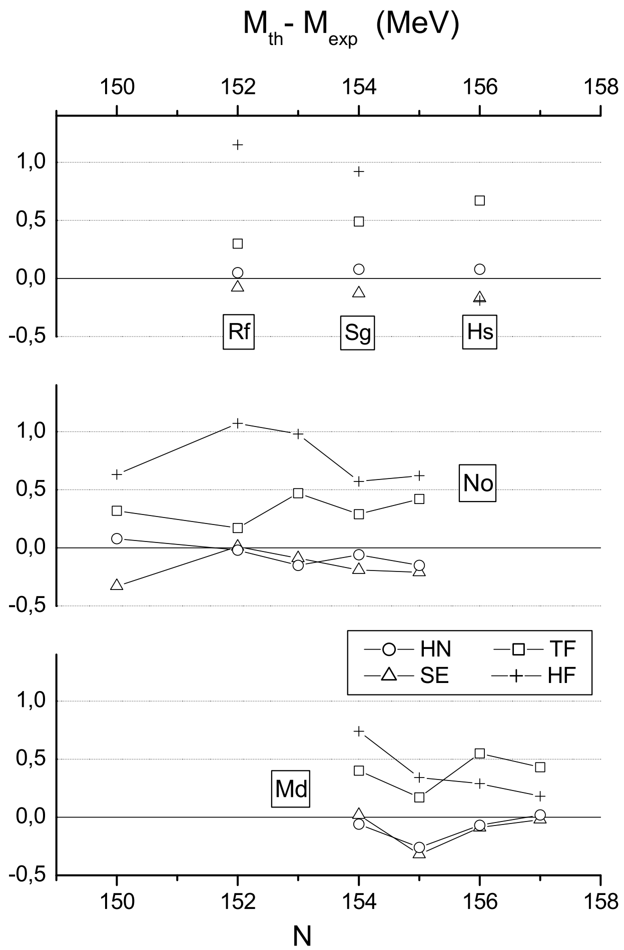

Figure 15: Differences between the SE, HN, TF and HF masses and experimental ones, for heaviest nuclei with Z=101-108 [45] (see text for the abbreviations).

ber Z=82 and assumed one Z=126 and with neutron number contained between known magic number N=126 and assumed one N=184. The macro-micro approximation HN is the model of the work [47], the same with which the calculated masses of Fig. 14 were obtained. The TF theory is the macro-micro model [48], in which the macroscopic part of mass was obtained with the use of the Thomas-Fermi approximation. Finally, the microscopic model HF is the Hartree-Fock-BCS approach [49], in which a 10-parameter Skyrme effective interaction has been used to obtain the mean field and a 4-parameter δ-function has been taken to describe the pairing interaction. Experimental masses used in Figs. 14 and 15 have been taken from [50]. One can see in Fig. 15 that the discrepancy between theoretical and experimental masses is roughly contained within ± 0.5 MeV for three of the considered models. Only for the HF approach, it is larger, up to about 1 MeV. The best agreement is obtained for the SE and HN approaches.

The α-decay energies, directly related with masses, are described with a similar accuracy as the masses [51].

5.4 Half-lives

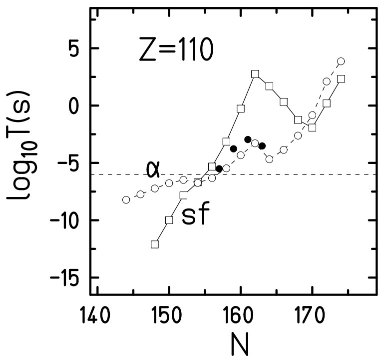

Figure 16: Comparison between predicted theoretically (open circles) and measured (full circles) α-decay half-lives, for isotopes of darmstadtium (Z=110) [52].

Fig. 16 shows an example of half-lives calculated for isotopes of darmstadtium (Ds, Z=110) [52]. The calculations are done for two main decay modes of heaviest nuclei: α decay (α) and spontaneous fission (sf), and the results are compared with experimental values. The latter are taken from [53] for ^{267}110, from [54] for ^{269}110 and ^{271}110 and from [55] for ^{273}110. One can see that the calculations correctly predicted the proper values of the half-lives and the mode of decay, i.e. the fact that the nuclei really undergo α decay and not fission.

6 Perspectives

Theoretical calculations of the half-lives (e.g. [58, 59]) indicate for a chance to observe many superheavy nuclei not seen up to the present. Also calculations of cross sections for the synthesis of them (e.g. [60–62]) indicate for such a chance.

In accordance with these, experiments aiming in the synthesis of new elements are planned. In Dubna (Russia), the element 117 is planned to be produced in the reaction [56]

$$^{50}\mathrm{Ti} \;+\; ^{243}\mathrm{Am} \;\rightarrow\; ^{293}117^{*}, \tag{3}$$

with the excited compound nucleus $^{293}117^{*}$ expected to emit 3 or 4 neutrons, leading to ^{290}117 or ^{289}117 evaporation residues. The elements 120 and 122 are also planned to be synthesized in Dubna in the reactions [56]

$$^{58}\mathrm{Fe} \;+\; ^{244}\mathrm{Pu} \;\rightarrow\; ^{302}120^{*} \;\rightarrow\; ^{299}120 \;+\; 3\mathrm{n}, \tag{4}$$

and

$$^{64}\mathrm{Ni} \;+\; ^{244}\mathrm{Pu} \;\rightarrow\; ^{308}122^{*} \;\rightarrow\; ^{305}122 \;+\; 3\mathrm{n}, \tag{5}$$

respectively.

The element 120 is also planned to be produced at GSI-Darmstadt (Germany) in another reaction [57]

$$^{64}\mathrm{Ni} \;+\; ^{238}\mathrm{U} \;\rightarrow\; ^{302}120^{*}, \tag{6}$$

with emission of 3 or 4 neutrons, leading to the nuclei ^{299}120 or ^{298}120, respectively.

There is much to be done with improvements of theoretical models which are used to describe the heaviest nuclei. A way to this are various tests of them, when describing detailed spectroscopic data obtained recently for as heavy nuclei as those with Z=102–106 (e.g. [63–65]).

The author would like to thank N.V. Antonenko, S.N. Dmitriev, S. Hofmann, Yu.Ts. Oganessian, K. Siwek-Wilczyńska and J. Wilczyński for helpful discussions. Support by the Polish Ministry of Science and Higher Education, grant No. 1 P03B 042 30, and the Polish-JINR(Dubna) Cooperation Programme is gratefully acknowledged.

References

[1] G.T. Seaborg, W.D. Loveland, *The elements beyond uranium*, J. Wiley, New York, 1990.

[2] A. Ghiorso, G.T. Seaborg, Prog. Part. Nucl. Phys. 31 (1993) 233.

[3] S. Hofmann, G. Münzenberg, Rev. Mod. Phys. 72 (2000) 733.

[4] P. Armbruster, Acta Phys. Pol. B 34 (2003) 1825.

[5] K.E. Gregorich et al., Phys. Rev. C 72 (2005) 014605.

[6] K. Morita et al., J. Phys. Soc. Jpn 76 (2007) 043201.

[7] Yu.Ts. Oganassian, J. Phys. G 34 (2007) R165.

[8] W.J. Świątecki, K. Siwek-Wilczyńska, J. Wilczyński, this issue.

[9] Yu.Ts. Oganassian, this issue.

[10] S.G. Nilsson, C.F. Tsang, A. Sobiczewski, Z. Szymański, S. Wycech, C. Gustafson, I.L. Lamm, B. Nilsson, Nucl. Phys. A 131 (1969) 1.

[11] M. Brack, J. Damgaard, A.S. Jensen, H.C. Pauli, V.M. Strutinsky, C.Y. Wong, Rev. Mod. Phys. 44 (1972) 320.

[12] M. Bolsterli, E.O. Fiset, J.R. Nix, J.L. Norton, Phys. Rev. C 5 (1972) 1050.

[13] A. Sobiczewski, A. Gyurkovich, M. Brack, Nucl. Phys. A 289 (1977) 346.

[14] P. Möller, J.R. Nix, Nucl. Phys. A 361 (1981) 117.

[15] D. Vautherin, D. M. Brink, Phys. Rev. C 5 (1972) 626.

[16] J. Dobaczewski, H. Flocard, J. Treiner, Nucl. Phys. A 422 (1983) 103.

[17] J. F. Berger, M. Girod, D. Gogny, Nucl. Phys. A 428 (1984) 23c.

[18] J.P. Delaroche. M. Girod, H. Goutte, J. Libert, Nucl. Phys. A 771 (2006) 103.

[19] P.-G. Reinhard, M. Rufa, J. Maruhn, W. Greiner, J. Friedrich, Z. Phys. A 323 (1986) 13.

[20] P. Ring, Prog. Part. Nucl. Phys. 37 (1996) 193.

[21] M. Bender, P.-H. Heenen, P.-G. Reihard, Rev. Mod. Phys. 75 (2003) 121.

[22] A. Sobiczewski, K. Pomorski, Prog. Part. Nucl. Phys. 58 (2007) 292.

[23] W.D. Myers, W.J. Swiatecki, Ark. Fys. 36 (1967) 343.

[24] K. Pomorski, J. Dudek, Phys. Rev. C 67 (2003) 044316.

[25] H.J. Krappe, J.R. Nix, A.J. Sierk, Phys. Rev. C20 (1979) 992.

[26] S. Ćwiok, J. Dudek, W. Nazarewicz, J. Skalski, T.Werner, Comput. Phys. Commun. 46 (1987) 379.

[27] V.M. Strutinski, Nucl. Phys. A 95 (1967) 420; Nucl. Phys. A 122 (1968) 1.

[28] Z. Patyk, A. Sobiczewski, P. Armbruster, K.-H. Schmidt, Nucl. Phys. A 491 (1989) 267.

[29] R. Smolańczuk, A. Sobiczewski, Proc. XV EPS Conf. on nuclear physics: *"Low Energy Nuclear Dynamics"*, St. Petersburg (Russia) 1995, ed. by Yu. Ts. Oganessian, W. von Oertzen and R. Kalpakchieva (World Scientific, Singapore, 1995) p. 313.

[30] Z. Patyk, A. Sobiczewski, Nucl. Phys. A 533 (1991) 132.

[31] Z. Patyk, A. Sobiczewski, Phys. Lett. B 256 (1991) 307.

[32] A. Sobiczewski, F.A. Gareev, B.N. Kalinkin, Phys. Lett. 22 (1966) 500.

[33] H. Meldner, Ark. Fys. 36 (1967) 593.

[34] U. Mosel, W. Greiner, Z. Phys. 222 (1969) 261.

[35] Z. Patyk, J. Skalski, A. Sobiczewski, S. Ćwiok, Nucl. Phys. A502 (1989) 591c.

[36] A. Sobiczewski, I. Muntian, Z. Patyk, Acta Phys. Slovaca 49 (1999) 83.

[37] S. Ćwiok, A. Sobiczewski, Z. Phys. A 342 (1992) 203.

[38] R.W. Hasse, W.D. Myers, *Geometrical Relationships of Macroscopic Nuclear Physics* (Springer, Berlin, 1988).

[39] A. Sobiczewski, Z. Patyk, S. Ćwiok, P. Rozmej, Nucl. Phys. A 485 (1988) 16.

[40] M. Warda, J.L. Egido, L.M. Robledo, Int. J. Mod. Phys. E 15 (2006) 504.

[41] I. Muntian, A. Sobiczewski, Acta Phys. Pol. B 32 (2001) 629.

[42] I. Muntian, Z. Patyk, A. Sobiczewski, Yad. Fiz. 66 (2003) 1051; Phys. At. Nucl. 66 (2003) 1015.

[43] I. Muntian, S. Hofmann, Z. Patyk, A. Sobiczewski, Acta Phys. Pol. B 34 (2003) 2073.

[44] I. Ragnarsson, A. Sobiczewski, R.K. Sheline, S.E. Larsson, B. Nerlo-Pomorska, Nucl.Phys. A233 (1974) 329.

[45] I. Muntian, Z. Patyk, A. Sobiczewski, APH N.S., Heavy Ion Physics 19 (2004) 139.

[46] S. Liran, A. Marinov, N. Zeldes, Phys. Rev. C 62 (2000) 047301.

[47] I. Muntian, Z. Patyk, A. Sobiczewski, Acta Phys. Pol. B 32 (2001) 691.

[48] W.D. Myers, W.J. Świątecki, Nucl. Phys. A 601 (1996) 141.

[49] F. Tondeur, S. Goriely, J.M. Pearson, M. Onsi, Phys. Rev. C 62 (2000) 024308.

[50] G. Audi, O. Bersillon, J. Blachot, A.H. Wapstra, Nucl. Phys. A 624 (1997) 1.

[51] A. Sobiczewski, I. Muntian, O. Parkhomenko, Proc. NATO Advanced Study Institute: *Structure and Dynamics of Elementary Matter*, Kemer (Turkey) 2003, eds. W. Greiner, M.G. Itkis, J. Reinhardt, M.C. Guclu (Kluwer Academic Publishers, Dordrecht, 2004) p. 377.

[52] A. Sobiczewski, Acta Phys. Pol. B 29 (1998) 2191.

[53] A. Ghiorso et al., Phys. Rev. C 51 (1995) 2293(R).

[54] S. Hofmann et al., Z. Phys. A 350 (1995) 277; A 350 (1995) 281.

[55] Yu.A. Lazarev et al., Phys. Rev. C 54 (1996) 620.

[56] Yu. Ts. Oganessian, S.N. Dmitriev, private commun. (2008).

[57] S. Hofmann, private commun. (2008).

[58] R. Smolańczuk, J. Skalski, A. Sobiczewski, Phys. Rev. C 52 (1995) 1871.

[59] R. Smolańczuk, Phys. Rev. C 56 (1997) 812.

[60] G.G Adamian, N.V. Antonenko, W. Scheid, Phys. Rev. C 69 (2004) 044601.

[61] W. Loveland, Phys. Rev. C 76 (2007) 014612.

[62] K. Siwek-Wilczyńska, A. Borowiec, I. Skwira-Chalot, J. Wilczyński, Int. J. Mod. Phys. E 17 (2008) 12.

[63] R.-D. Herzberg, J. Phys. G 30 (2004) R123.

[64] F.P. Hessberger et al., Eur. Phys. J. A 29 (2006) 281.

[65] A. Lopez-Martens et al., Phys. Rev. C 74 (2006) 044303.